Clonal analysis reveals multiple functional defects of aged murine hematopoietic stem cells

Brad Dykstra,[1,2] Sandra Olthof,[1] Jaring Schreuder,[1] Martha Ritsema,[1,2] and Gerald de Haan[1,2]

[1]Department of Cell Biology; and [2]Stem Cell Biology Laboratory, European Research Institute on the Biology of Aging; University Medical Center Groningen, University of Groningen, 9700 RB Groningen, Netherlands

Hematopoietic stem cell (HSC) populations change with aging, but the extent to which this is caused by qualitative versus quantitative alterations in HSC subtypes is unclear. Using clonal assays, in this study we show that the aging HSC compartment undergoes both quantitative and qualitative changes. We observed a variable increase of HSC pool size with age, accompanied by the accumulation of predominantly myeloid–biased HSCs that regenerate substantially fewer mature progeny than young myeloid–biased HSCs and exhibit reduced self–renewal activity as measured by long-term secondary transplantation. Old HSCs had a twofold reduction in marrow–homing efficiency and a similar decrease in functional frequency as measured using long-term transplantation assays. Similarly, old HSCs had a twofold reduced seeding efficiency and a significantly delayed proliferative response compared with young HSCs in long-term stromal cell co-cultures but were indistinguishable in suspension cultures. We show that these functional defects are characteristics of most or all old HSCs and are not indicative of a nonfunctional subset of cells that express HSC markers. Furthermore, we demonstrate that cells with functional properties of old HSCs can be generated directly from young HSCs by extended serial transplantation, which is consistent with the possibility that they arise through a process of cellular aging.

CORRESPONDENCE
Brad Dykstra:
b.j.dykstra@med.umcg.nl
OR
Gerald de Haan:
g.de.haan@med.umcg.nl

Abbreviations used: CAFC, cobblestone area–forming cell; HSC, hematopoietic stem cell; MPP, multipotent progenitor.

Organismal aging is accompanied by a general decline in many tissues and organs. With few exceptions, specialized cells in the body have a limited lifespan, and therefore tissues must be maintained and regenerated by resident tissue-specific stem cells. By extension, much of the age-related decline in tissue function and related pathologies may be attributed to changes in these stem cell pools over time. Stem cell aging likely involves genetic mutations and alterations at the epigenetic and protein levels in the stem cells themselves, in combination with changes in the aged microenvironment in which the stem cells reside. The relative contributions of each of these factors continue to be important areas of research and debate (Liu and Rando, 2011). A more complete understanding of the biology and mechanisms of stem cell aging could enable targeted treatment strategies aimed to reduce or even reverse the aging process at the stem cell level as a strategy to combat aging and age-related pathologies.

The murine hematopoietic system is probably the best-studied model of mammalian stem cell aging. It has long been appreciated that the hematopoietic stem cell (HSC) activity of BM cells from young and old mice is different. Transplants of old BM were shown to outperform the same number of cells from young mice (Harrison, 1983), and this was later determined to be caused by an age-related increase in the concentration of HSCs in the BM (Harrison et al., 1989). The advent of flow cytometry and subsequent discovery of cell surface markers that enrich for functionally defined HSCs soon led to the realization that the size of the stem cell pool, as defined by any of a variety of marker combinations, increases dramatically with age (Morrison et al., 1996; Sudo et al., 2000; Rossi et al., 2007b). However, although

a similar proportion of these cells purified from old or young mice were functional when measured in vitro, a markedly reduced frequency of purified cells from old mice was deemed to be functional HSCs when measured in long-term transplantation assays (Morrison et al., 1996; Sudo et al., 2000). These observations led to two early hypotheses; namely, that the pool of cells expressing HSC-associated markers is contaminated with primitive progenitors that are detected by in vitro assays but lack repopulating ability in vivo (Sudo et al., 2000) or that HSCs from old mice have a homing and/or engraftment defect and therefore remain undetected (Morrison et al., 1996). The former hypothesis is supported by observations of improved functional frequencies when alternate marker combinations are used to purify old HSCs (Yilmaz et al., 2006). Support for the latter is provided by a study of short-term HSC homing that reported a twofold lower ability of functionally defined HSCs from old mice to home to the BM or spleen within a 24 h period (Liang et al., 2005). In addition, there is now strong evidence of age-related differences in the properties of HSCs that do engraft in vivo (Dykstra and de Haan, 2008). The best characterized of these differences is that upon transplantation; old HSCs tend to have a myeloid-skewed blood cell production caused by a decreased ability to produce lymphoid cells (Sudo et al., 2000; Kim et al., 2003; Liang et al., 2005; Rossi et al., 2005; Cho et al., 2008; Beerman et al., 2010a).

Functional changes occurring in the HSC pool with age have been commonly attributed to cellular aging. According to this model, the functional properties of individual HSCs gradually decline as the result of an accumulation of cellular damage such as the accrual of DNA lesions (Rossi et al., 2007a; Mohrin et al., 2010; Yahata et al., 2011) or epigenetic dysregulation (Bennett-Baker et al., 2003; Chambers et al., 2007). However, the identification of separate populations of intrinsically lineage-biased HSCs (Müller-Sieburg et al., 2002; Dykstra et al., 2007) has suggested a different model in which the clonal composition of the HSC pool, rather than individual HSCs, changes with age. Specifically, myeloid-dominant HSCs are thought to accumulate in the old HSC pool at the expense of lymphoid-dominant and lineage-balanced HSCs (Cho et al., 2008; Muller-Sieburg and Sieburg, 2008; Beerman et al., 2010a; Challen et al., 2010). In this latter model, individual HSCs from old mice are thought to be functionally equivalent to their lineage-biased counterparts in young mice, and as such, age-associated differences in the function of the HSC compartment are thought to be caused exclusively by the relative increase in myeloid-dominant HSCs. (Cho et al., 2008; Muller-Sieburg and Sieburg, 2008; Challen et al., 2010). Although these models are not mutually exclusive, determining their respective significance is a vital step toward a complete understanding of the underlying mechanisms.

Resolution of these issues has to date been confounded by difficulties in interpreting the results of assays of bulk populations of old and young HSCs, which preclude assessments of heterogeneity within these HSC compartments. In a recent study in which clonal analysis was performed by transplanting limiting dilutions of unseparated or lineage-depleted BM cells (Cho et al., 2008), it was determined that the relative proportion of myeloid-dominant HSCs increases with age and that myeloid-dominant HSCs from both young and old mice show a blunted IL-7 response. More recently, Beerman et al. (2010a) reported that myeloid-dominant HSCs were enriched in the CD150^{hi} population of LSK CD34^{−}flt3^{−} BM and that the size of this population increased dramatically with age. Furthermore, when populations of purified CD150-matched HSCs from old and young donors were compared in primary and secondary competitive transplants, a significant decrease in the output of mature cells from old HSCs was observed (Beerman et al., 2010a). However, because a comprehensive analysis of the functional properties of individual old and young HSCs is lacking, the identity of any functional changes in individual old HSCs remains elusive.

In this study, we set out to obtain a more complete and high-resolution understanding of the aging HSC pool. To do this, we designed a series of experiments to evaluate multiple properties of purified HSCs isolated from the BM of young and old mice. Collectively, our analyses reveal that a population of predominantly myeloid-dominant HSCs accumulates with age and that individual old HSCs are functionally inferior to their young counterparts in multiple parameters, including a lower functional frequency in vitro and in vivo, a delayed proliferation response in stromal co-cultures, a reduced efficiency for short-term BM homing, production of smaller clones of mature cells in transplanted recipients, and a reduced long-term in vivo self-renewal activity. Furthermore, we present evidence that in vivo repopulating cells with characteristics of aged HSCs can be generated from young HSCs over a prolonged course of a serial transplantation similar in duration to the lifespan of a mouse.

RESULTS

The frequency of BM cells with HSC markers increases dramatically with age but is highly variable between individual old mice

The overall proportion of BM cells expressing HSC-associated cell surface markers has been reported to increase with age in the mouse (Dykstra and de Haan, 2008). To confirm this, we stained BM from 10 young (4–5 mo old) and 22 old (24–28 mo old) C57BL/6 (B6) mice with a panel of HSC markers (Fig. 1 A). Consistent with earlier studies (Morrison et al., 1996; Sudo et al., 2000; Rossi et al., 2007b), the median proportion of Lin^{lo}Sca1^{+}cKit^{+} (LSK) cells within the BM increased 1.9-fold in old mice (Fig. 1 B), and the proportion of CD48^{−}CD34^{−}EPCR^{+}CD150^{+} (48^{−}34^{−}E^{+}150^{+}) cells within the LSK increased a further 4.6-fold (Fig. 1 C). Collectively, we observed a mean 12-fold increase in the frequency of LSK48^{−}34[−]E[+]150^{+} cells in old mice (Fig. 1 D). However, although the frequency of BM cells with HSC markers was similar in all young mice (i.e., 75–100 cells per million), these frequencies were highly variable between old individuals, ranging from 100 to 4,300 LSK48^{−}34[−]E[+]150^{+} cells per million viable
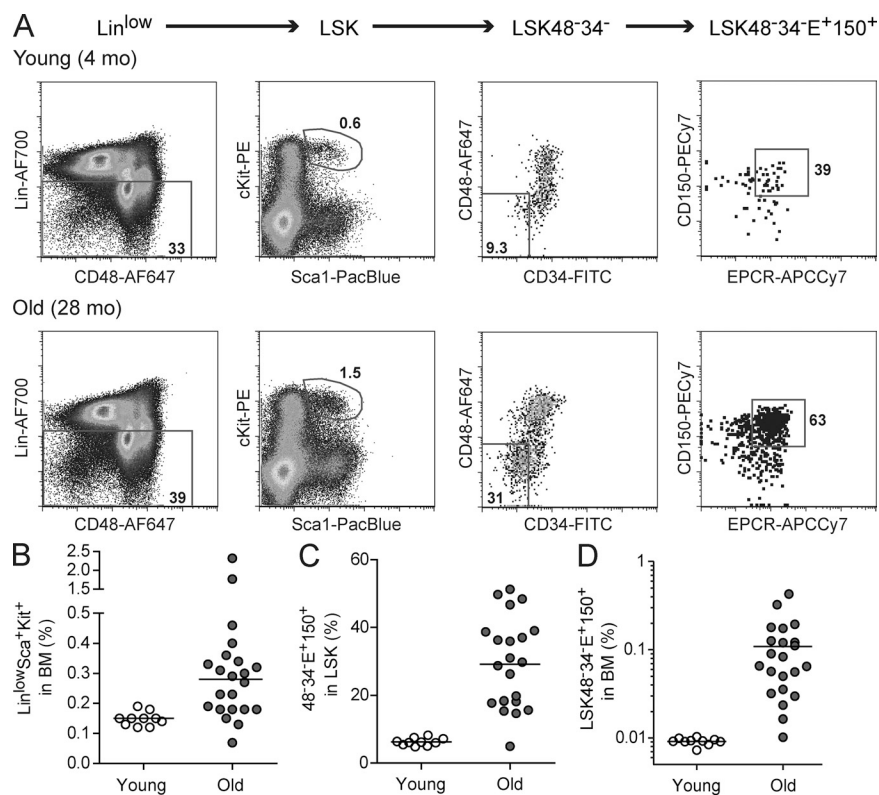
Figure 1. The frequency of BM cells with HSC markers increases with age but is highly variable between individual old mice. (A) Representative FACS profiles of BM from young and old mice. BM from a young (4 mo) and an old (28 mo) mouse was collected and stained with antibodies specific for HSC markers as described in Materials and methods. Equal numbers of events (4.5×10^5) are shown for each mouse. Viable cells were first selected based on their forward and side scatter properties and their exclusion of propidium iodide. Lineage-low (Lin^{lo}) cells were then selected as shown in the leftmost panel, followed by gating for cells double positive for Sca1 and cKit to identify the LSK population. The LSK population was enriched further by selecting those cells negative for CD34 and CD48 and positive for EPCR (E$^+$) and CD150 to obtain the stem cell–enriched LSK48$^-$34$^-$E$^+$150$^+$ population. (B and C) Percentage of Lin^{lo}Sca1$^+$cKit$^+$ (LSK) in BM and percentage of CD48$^-$CD34$^-$EPCR$^+$CD150$^+$ within the LSK population of 10 individual young (4–5 mo) and 22 old (24–28 mo) mice. Dots represent individual mice, and horizontal lines indicate median values. (D) Mean BM frequencies of LSK48$^-$34$^-$E$^+$150$^+$ cells in the same 10 young and 22 old mice.

BM cells. Therefore, young mice exhibit strict control of the LSK48$^-$34$^-$E$^+$150$^+$ pool size, whereas in old mice this is much less evident.

Old LSK48$^-$34$^-$E$^+$150$^+$ cells have reduced clonogenic efficiency in stromal co-cultures but not in liquid cultures

Together with the dramatic increase in cells with HSC markers in old BM, it is also well established that this population has, on average, a reduced function per cell compared with young cells with the same marker combination (Beerman et al., 2010b). However, a full understanding of this phenomenon requires analysis of individual HSCs. For example, old cells with HSC markers might all have a similar but reduced function compared with their young counterparts. Alternatively, this population of cells in old mice might simply reflect the presence in the sorted population of functionally unrelated cells that express the same combination of surface molecules. To address this, we first compared at a clonal level the proliferative response of various purified cell populations from young and old mice in stromal cell–containing and stroma-free cultures.

When single cells were seeded in stroma-free cytokine-supplemented cultures, ∼90% of LSK48$^-$34$^-$E$^+$150$^+$ cells and ∼80% of LSK48$^-$150$^+$ cells demonstrated extensive proliferative potential in response to stem cell factor plus IL-11, regardless of the age of the mouse from which they had been obtained (Fig. 2 A). This indicates that the phenotypically defined HSC compartment in old mice is not contaminated with cells that are completely nonfunctional. Indeed, when exposed to high levels of mitogenic cytokines, virtually all single cells of the sorted populations exhibited a considerable proliferative response.

Next, we compared the clonogenic efficiency of purified cells using a complementary in vitro assay that is closer to physiological conditions in that it relies on stromal feeder cells without the addition of recombinant cytokines. Single purified cells were sorted onto preestablished FBMD-1 (Flask BM Dexter-1; FBMD) stromal feeder layers and were scored for their ability to generate characteristic "cobblestone" colonies at any point on or after day 7. The proportion of single cells thus classified as cobblestone area–forming cells (CAFC [CAFCd7+]) was found to be almost twofold lower in old compared with young LSK48$^-$34$^-$E$^+$150$^+$ cells (Fig. 2 B, left bars). Of interest, this defect appeared to be specific to the cells with HSC-associated markers because no difference in CAFC frequency in LSK48$^+$150$^-$ cells (which contain hematopoietic progenitors but no HSC activity) from young and old mice was detected (Fig. 2 B, right bars). Consistent with this, a similar analysis of LSK48$^-$150$^+$ cells, which contain CD34$^+$ and EPCR$^-$ cells in addition to LSK48$^-$34$^-$E$^+$150$^+$ cells, demonstrated an intermediate (1.5-fold) decrease in CAFC frequency with age (Fig. 2 B, middle bars).

It is important to note that the proportion of old LSK48$^-$34$^-$E$^+$150$^+$ cells that were functional as measured in this CAFC assay had no correlation with their frequency in individual old mice (Fig. 2 C). This indicates that the increased variation in the primitive cell pool size observed in old mice is independent of the accompanying functional decline in the
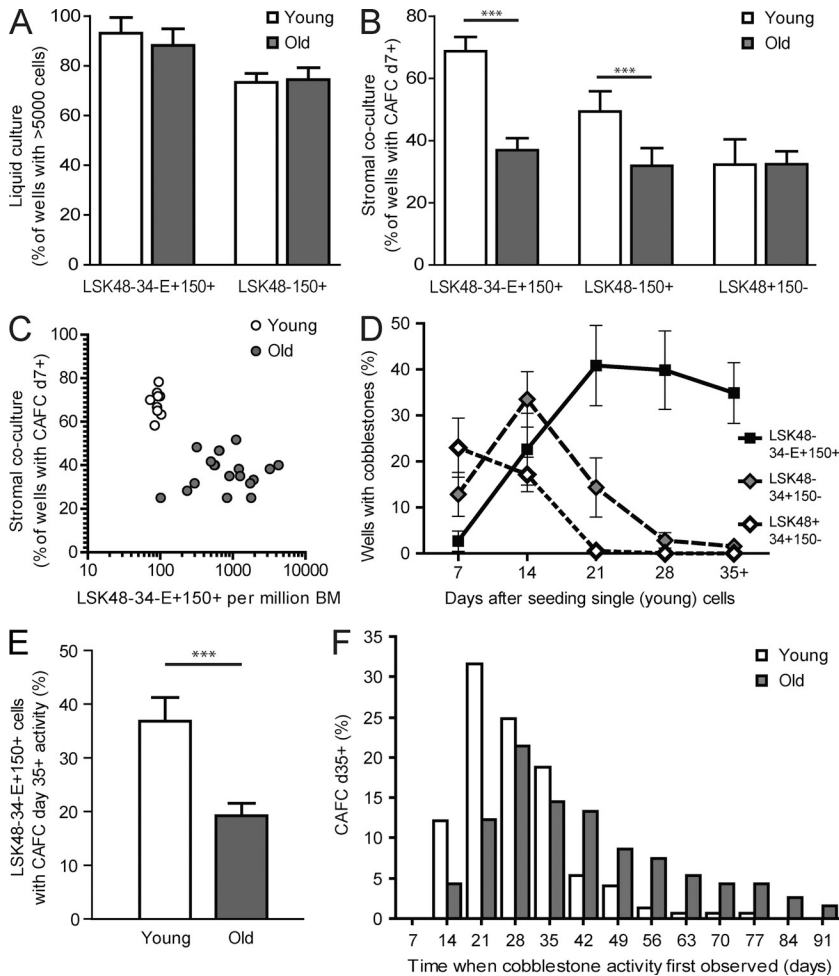
Figure 2. Old and young BM cells with HSC markers have similar clonogenic ability in liquid culture but have reduced activity in stromal co-cultures. (A) 60–120 purified Lin^{lo}Sca1$^+$cKit$^+$CD48$^-$CD34$^-$EPCR$^+$CD150$^+$ (LSK48$^-$34$^-$E$^+$150$^+$) and LSK48$^-$150$^+$ cells from each of five young or six old mice were seeded individually as single cells into liquid cultures supplemented with stem cell factor and IL-11. Shown is the mean proportion of single purified cells from the individually tested young and old mice that generated clones of at least 5,000 cells within 2 wk of culture. (B) 60–120 purified LSK48$^-$34$^-$E$^+$150$^+$, LSK48$^-$150$^+$, and LSK48$^+$150$^-$ cells from young or old mice were seeded as single cells onto FBMD stroma and scored weekly for the presence or absence of cobblestone areas. Shown is the mean proportion of single purified cells from individually tested young (n = 7–9) and old (n = 12–20) mice that generated cobblestone areas at day 7 or later (CAFCd7+). (C) Dots represent individual young (n = 9) or old (n = 19) mice and show the size of the LSK48$^-$34$^-$E$^+$150$^+$ pool (as described in Fig. 1) and the clonogenic efficiency in stromal co-culture (as shown in B). (D) LSK48$^-$34$^-$E$^+$150$^+$ (HSC containing), LSK48$^-$34$^+$150$^-$ (more primitive MPPs), and LSK48$^+$34$^+$150$^-$ (less primitive MPPs) were isolated from young BM and seeded individually onto FBMD stroma and scored weekly for the presence or absence of cobblestone areas, which are characteristic of proliferating primitive cells. Data represent a minimum of 500 wells per cell type from a total of 10 individual young mice. (E) 60 purified LSK48$^-$34$^-$E$^+$150$^+$ cells from each of 9 young and 19 old mice were seeded individually as single cells onto FBMD stroma and scored weekly for 11–13 wk for the presence or absence of cobblestone areas. Shown is the mean proportion

of single purified LSK48$^-$34$^-$E$^+$150$^+$ cells from the individually tested young and old mice that generated cobblestone areas at any time point day 35 or later (CAFCd35+). (F) Proportion of LSK48$^-$34$^-$E$^+$150$^+$ cells with CAFCd35+ activity (described in E) that first generated cobblestone areas at the specified time after seeding. P < 0.001 for old (n = 187) versus young (n = 149) CAFCd35+, Mann-Whitney U test. Error bars on all panels represent 95% confidence intervals of the mean. ***, P < 0.001, unpaired two-tailed Student's t test.

stem cell pool. Considering the wide range in LSK48$^-$34$^-$E$^+$150$^+$ cell frequency between individual old mice (Fig. 1 D), this reveals that the size of the functional HSC pool can vary almost 50-fold between genetically identical mice of advanced age.

Reduced frequency and delayed proliferation response of CAFC day 35+ in LSK48$^-$34$^-$E$^+$150$^+$ population from old BM

We then compared the frequency and properties of functional HSCs within young and old LSK48$^-$34$^-$E$^+$150$^+$ cells using an in vitro assay for HSC activity. In the FBMD stromal co-cultures just described, the timing of cobblestone generation corresponds to the primitive status of the initiating cell (Breems et al., 1994; de Haan et al., 1997). For example, day 7–10 CAFC (CAFCd7-10) activity overlaps with hematopoietic progenitors as measured by early spleen colony–forming ability, whereas CAFCd28-35 activity overlaps with HSC activity as measured by long-term in vivo repopulation assays

(Ploemacher et al., 1991; Neben et al., 1993). Because each culture was initiated with a single purified cell, we could measure the commencement and duration of cobblestone ability at a clonal level. In the experiments described here, we considered the ability to generate cobblestones at day 35 or later (CAFCd35+) as a surrogate measurement for HSC activity. To confirm the utility of this measurement, we sorted three LSK subpopulations from young BM: LSK48$^-$34$^-$E$^+$150$^+$, LSK48$^-$34$^+$150$^-$, and LSK48$^+$34$^+$150$^-$, which are known to contain HSCs, more primitive multipotent progenitors (MPPs), and less primitive MPPs, respectively (Wilson et al., 2008). When single cells of these phenotypes were measured using the CAFC assay, clear differences in the timing of cobblestone generation were observed, with CAFCd35+ activity restricted almost entirely to the most primitive LSK48$^-$34$^-$E$^+$150$^+$ cells (Fig. 2 D).

60 LSK48$^-$34$^-$E$^+$150$^+$ cells from each of 9 young and 19 old mice were individually seeded onto preestablished stromal layers and scored weekly for cobblestone activity for up

to 13 wk. Of interest, out of >3,000 individual young and old LSK48⁻34⁻E⁺150⁺ and LSK48⁻150⁺ cells tested, cobblestone activity was never observed to disappear one week and reappear at a later week. The frequency of LSK48⁻34⁻E⁺150⁺ cells that generated cobblestones at day 35 or later (CAFCd35+) was found to be 1.9-fold lower in old than young mice (Fig. 2 E). Furthermore, the CAFCd35+ cells from young and old mice also exhibited distinct growth properties. Most young CAFCd35+ cells first generated cobblestones at day 21–28, and only 13% were first observed beyond 35 d. In contrast, old CAFCd35+ showed a significantly delayed response, with almost half (48%) generating no observable cobblestones until after 35 d and a sizeable fraction (12%) delayed until week 10 or later (Fig. 2 F).

Reduced functional HSC frequency in the LSK48⁻34⁻E⁺150⁺ population from old BM as measured by long–term limiting dilution transplantations

We then quantified the frequency of functional HSCs within the LSK48⁻34⁻E⁺150⁺ populations from young and old donors by determining their ability to regenerate blood formation in a long-term limiting dilution transplantation assay. We injected five purified LSK48⁻34⁻E⁺150⁺ cells from young or old donors into 63 and 143 young recipients, respectively (Fig. 3 A). From the proportions of recipients with significant (>1%) donor contribution to circulating granulocytes (Gr-1⁺SSCʰⁱ) at 24 wk after transplant (46/63 recipients of young cells and 65/143 recipients of old cells), we calculated the frequencies of functional HSCs in the starting populations to be 2.2-fold lower in the old versus young LSK48⁻34⁻E⁺150⁺ cells (26% vs. 12%; Fig. 3 B). However, considering the mean 12-fold increase in LSK48⁻34⁻E⁺150⁺ frequency in old mice (Fig. 1 D), this still represents a more than fivefold mean increase in the size of the functional HSC pool between 5 and 24 mo of age.

LSK48⁻150⁺ cells from old mice have reduced short–term BM–homing efficiency

One possible explanation for the reduced in vivo functional frequency of old LSK48⁻34⁻E⁺150⁺ cells is that these cells exhibit an age-dependent change in their homing properties. The only previous study that tested the short-term homing efficiency between young and old HSCs (Liang et al., 2005) did so on a purely functional basis, by measuring the competitive repopulating unit (CRU) content of whole BM before and after homing into irradiated recipients using secondary-transplantation assays. Although this is a relevant and informative approach, it is limited in that it measures homed cells indirectly, using a second assay that itself is dependent on homing. To more directly and definitively measure whether changes in physical homing efficiency could be responsible for the effects observed here, we compared the short-term homing ability of purified cells from old and young mice (Fig. 4 A). To do this, we purified LSK48⁻150⁺ cells from old and young mice transgenic for CFP, GFP, or dsRed, combined them at a known ratio, and injected them into

irradiated recipients. 16–21 h later, the recipients were sacrificed, and the ratio of fluorescent cells obtained from the BM was compared with the ratio in which they were injected (Fig. 4 A). This approach allowed the relative homing efficiency of young and old cells to be measured directly, that is, in the same recipient. The results clearly showed that the short-term marrow-homing efficiency of old LSK48⁻150⁺ was reduced almost twofold compared with the coinjected young LSK48⁻150⁺ cells (Fig. 4 B).

Defective in vivo homing and reduced growth on stromal cells in vitro are not shared features of old LSK48⁻150⁺ cells

The similar magnitudes of the in vivo homing defect and reduction in CAFC efficiency suggested that these properties might be associated. Specifically, we hypothesized that there might be a subset of cells in old mice that express HSC markers (Fig. 1) and can proliferate in response to high levels of recombinant cytokines (Fig. 2 A) but are functionally deficient, both in short-term homing (Fig. 4 B) and in response to stromal co-culture (Fig. 2 B). To determine whether the LSK48⁻150⁺ cells with homing defects are the same as those that lack CAFC activity in stromal co-cultures, we compared the CAFCd7+ efficiency of old and young cells isolated before and after homing. However, this analysis revealed no functional improvement in homed old LSK48⁻150⁺ cells as compared with young LSK48⁻150⁺ cells (Fig. 4 C), suggesting that the poor homing of the old cells and poor growth in stromal co-cultures are nonoverlapping features of the same cells. Thus, there does not appear to be a contaminating subfraction within the old LSK48⁻150⁺ population that is completely nonfunctional. Rather, this observation is consistent with the notion that these two functional defects are randomly distributed across the old HSC pool or that they may be general characteristics of all old HSCs.

LSK48⁻34⁻E⁺150⁺ BM cells from old mice contain an increased proportion of myeloid–dominant HSCs with a lower output of mature blood cells per HSC

We next compared the functional characteristics of individual young and old HSCs upon transplantation into irradiated hosts. To do this, we began with the set of 111 positive recipients that were transplanted at limiting dilution with five old or young LSK48⁻34⁻E⁺150⁺ cells and performed self-renewal, lineage distribution, and blood cell output measurements in primary, secondary, and tertiary transplanted mice, as shown schematically in Fig. 3 A. As a strict measure for long-term, active hematopoiesis, we considered a mouse to be transplanted with an HSC only if there was a minimum 1% donor contribution to the short-lived (Pillay et al., 2010) granulocyte population (defined as Gr-1⁺SSCʰⁱ) at 24 wk after transplant. This is a more stringent definition than is normally applied and would be expected to exclude virtually all clones in which robust self-renewal had not occurred (Dykstra et al., 2007; Kent et al., 2009). At the same time, we did not stipulate minimum levels of donor-derived lymphoid
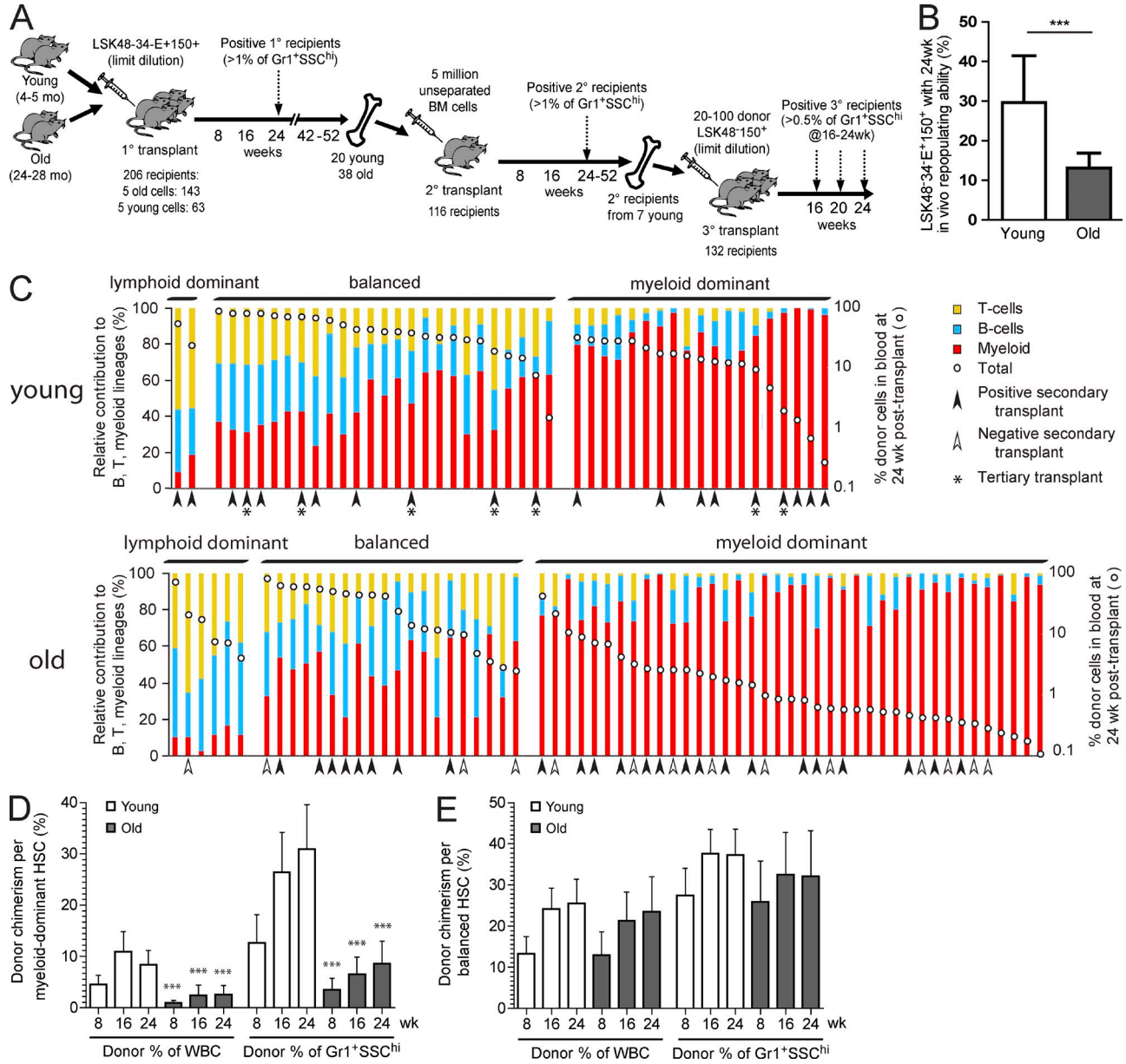
Figure 3. The old LSK48⁻34⁻E⁺150⁺ HSC pool is reduced in functional frequency and contains an increased proportion of myeloid–dominant HSCs with a lower output per HSC. (A) Summary of serial transplantation experiments designed to test lineage contribution ratio, overall blood cell output, and in vivo self-renewal properties of individual young and old HSCs. Data from primary (1°), secondary (2°), and tertiary (3°) recipients are presented in Figs. 3, 5, and 6, respectively. (B) Five old or young LSK48⁻34⁻E⁺150⁺ cells were transplanted into 206 lethally irradiated young recipients, as described in Materials and methods. Positive recipients (46/63 young, 65/143 old) were defined as those with >1% donor contribution to circulating granulocytes (Gr-1⁺SSCʰⁱ) at 24 wk after transplant, and functional HSC frequency was estimated via limiting dilution calculation. Calculated HSC frequencies were 1 in 3.8 and 1 in 8.3 for young and old LSK48⁻34⁻E⁺150⁺ cells, respectively. Error bars represent 95% confidence interval. ***, P < 0.001, likelihood ratio test. (C) Relative lineage contribution and overall donor contribution levels in all positive primary recipients. Positive recipients (46 young and 65 old) were classified as myeloid dominant, balanced, or lymphoid dominant based on the relative donor contribution ratio to circulating B, T, and myeloid cells at 24 wk after transplant, as described in Materials and methods. Each bar represents a positive mouse, and the red, blue, and yellow segments represent the relative donor contributions to the myeloid, B, and T lineages in the peripheral blood at 24 wk after transplant. Total donor contribution to the peripheral blood is indicated by the white dot for each mouse and is plotted using the logarithmic secondary y axis. Arrowheads indicate those primary recipients that were used as donors for secondary transplants. Asterisks indicate those primary recipients that were used as donors for secondary and tertiary transplants. (D and E) The mean contribution to total peripheral blood or to the granulocyte (Gr-1⁺SSCʰⁱ) lineage was determined for myeloid-dominant (young n = 19, old n = 39) or balanced (young n = 25, old n = 20) primary recipients of young or old LSK48⁻34⁻E⁺150⁺ HSCs. To determine the donor chimerism per myeloid-dominant or balanced HSC, these mean contributions were corrected for differences in starting HSC frequency by dividing by the mean number of functional HSCs injected per positive recipient (1.79 HSCs per positive young recipient and 1.33 HSCs per positive old recipient). Time is indicated in weeks after transplant. Error bars represent 95% confidence intervals. All pairs were significantly different (***, P < 0.001) at the same time point between young and old for myeloid-dominant HSCs, and no significant differences were found for balanced HSCs (Mann-Whitney U test).
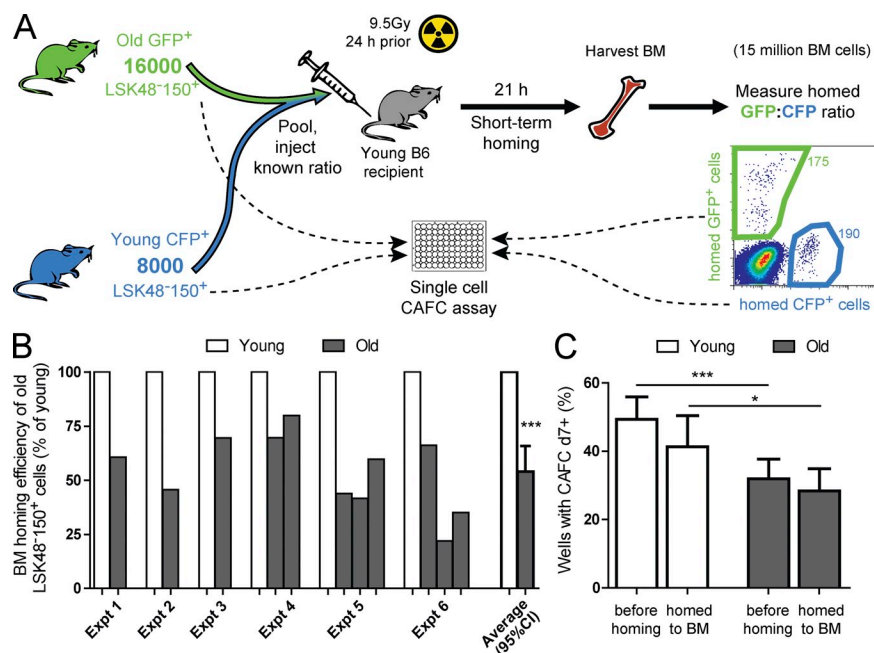
Figure 4. **LSK48⁻150⁺ cells from old mice have reduced short-term marrow-homing efficiency compared with LSK48⁻150⁺ cells from young mice.** (A) Setup of short-term homing experiment. Shown here is a representative example (corresponding to experiment 2 in B). (B) Short-term BM-homing efficiency of old relative to young LSK48⁻150⁺ cells. Results from six independent experiments are shown. In experiments 4–6, more than two distinguishable donor cell types were transplanted simultaneously. (C) CAFC efficiency of young and old LSK48⁻150⁺ cells before and after homing. 30–120 individual LSK48⁻150⁺ cells from the old and young donors in B, either freshly isolated or isolated from the BM of short-term homing recipients, were seeded in stromal co-cultures and checked weekly for cobblestone areas. Shown is the mean proportion of single purified cells from 6 young mice and 11 old mice that generated cobblestone areas at day 7 or later (CAFCd7+). Error bars indicate 95% confidence interval of the mean (CI). *, P < 0.05; ***, P < 0.001, two-tailed Student's *t* test.

cells or overall donor cells in the blood. This decision was taken to ensure that any cells with robust self-renewal potential but lacking appreciable lymphoid differentiation potential, as have been reported to exist in both young (Dykstra et al., 2007; Morita et al., 2010) and old mice (Sudo et al., 2000), would not be excluded.

It is important to note that although the primary recipients were injected with limiting dilutions of purified cells, they were not strictly equivalent to single-cell transplants because there is a certain likelihood that some positive mice were engrafted with multiple HSCs. Based on the estimated frequency obtained by limiting dilution calculations (Fig. 3 B), it could be expected that half of the positive mice transplanted with five young LSK48⁻34⁻E⁺150⁺ cells would have been clonally repopulated, 30% with two HSCs, and 20% with three or more HSCs. For the recipients of five old LSK48⁻34⁻E⁺150⁺ cells, >70% of positive recipients would be expected to have been clonally repopulated and only 6% with three or more HSCs.

First we compared the lineage distribution patterns of donor-derived blood cells in all positive primary recipients. To categorize the lineage distribution patterns, we calculated the ratio of the donor contribution to myeloid, B, and T lineage cells in each mouse at 24 wk after transplant. Using this ratio, we classified the outputs as myeloid dominant (α like), lymphoid dominant (γ like), or balanced (β like; Fig. 3 C), according to the terms previously assigned to similar definitions of these patterns (Dykstra et al., 2007). As expected (Dykstra et al., 2007; Cho et al., 2008; Beerman et al., 2010a), a balanced lineage output was the most common pattern in the recipients of young HSCs, whereas a myeloid-dominant lineage output was the most common pattern in the recipients of old HSCs. Lymphoid-dominant repopulation was rarely seen in this dataset. This is likely because of our use of a sorting strategy

that excluded CD150⁻ cells (Kent et al., 2009; Beerman et al., 2010a; Morita et al., 2010) and a strict requirement for donor-derived granulocyte production at 24 wk after transplant to score mice as positive.

Overall repopulation levels per repopulated mouse were noticeably different between recipients of young and old donor HSCs, particularly in the recipients with myeloid-dominant donor contributions. Of the myeloid-dominant recipients of old HSCs, more than half (22 of 39) had overall donor contributions of <1% in the blood at 24 wk after transplant, in contrast to only 2 of 19 such cases in recipients of young HSCs (Fig. 3 C). Even after correction for differences in the mean number of functional HSCs injected, the donor-derived blood cell output per old myeloid-dominant HSC was found to be significantly reduced at all time points tested (Fig. 3 D). In contrast, there was no significant difference in overall output or granulocyte production between balanced HSCs from old or young donors (Fig. 3 E). These results clearly show that the myeloid-dominant HSCs that accumulate in old mice are functionally distinct from those that are present in young mice.

Old HSCs have decreased self-renewal activity and generate smaller daughter clones in extended serial transplants

Next, we performed secondary transplantations using cells from 58 primary recipients that had been transplanted with limiting dilutions of young or old HSCs to compare their self-renewal activity in vivo. At 10–12 mo after transplant, these primary recipients (identified by arrowheads in Fig. 3 C) were sacrificed, and 5 million unseparated BM cells were transplanted into pairs of secondary recipients. Positive secondary recipients were identified using the same stringent definition as was used for the primary recipients (>1% donor contribution to circulating Gr-1⁺SSC^hi granulocytes at 24 wk

after transplant), and the presence of at least one positive secondary recipient was used as an indication that the originally transplanted HSC had extensive and long-term self-renewal activity in vivo. 20 of 20 mice transplanted with young HSCs successfully repopulated secondary recipients in this assay, compared with only 24 of 38 mice transplanted with old HSCs. Notably, the old HSCs with limited self-renewal ability did not correlate with a particular lineage distribution pattern or overall repopulation level (Fig. 3 C and Table I). After correcting for differences in the mean number of functional HSCs injected per primary recipient, the estimated proportion of primary HSCs with extensive self-renewal activity was determined to be ~44% lower for old HSCs than young HSCs (Fig. 5 A). Repopulated secondary recipients of both old and young HSCs tended to recapitulate the lineage contribution pattern seen in primary recipients (Fig. 5 B). Furthermore, even after correcting for differences in the original HSC number injected, the output of blood cells per primary HSC in secondary recipients was found to be significantly lower when derived from old donor HSCs than from young HSCs. In contrast to the output in primary recipients (Fig. 3, D and E), the reduced blood cell output in secondary recipients was observed for all old HSCs, regardless of their original lineage contribution pattern (Fig. 5, C and D).

Cellular origins of aged HSCs

Finally, we wanted to gain insight into the origins of the low–output myeloid-dominant HSCs that accumulate with age. Specifically, we wondered whether these cells might arise from normal young HSCs or whether they are a unique type of epigenetically fixed HSCs present in young mice at low numbers but accumulating with age because of differences in proliferation or self-renewal. To answer this question, we aged young HSCs over 18–24 mo in vivo through

primary and secondary transplantations and then repurified donor-derived HSCs and injected them at limiting dilutions into tertiary recipients (Fig. 3 A). 16–24 wk later, the tertiary recipients were analyzed for donor-derived cells in the peripheral blood (Table II). Almost all positive tertiary recipients were myeloid dominant and had low levels of overall chimerism, reminiscent of the myeloid-dominant HSCs that accumulate with age (Fig. 6). This demonstrates that HSCs with characteristics of those found in aged mice can be generated from normal young HSCs within the lifetime of a mouse.

DISCUSSION

Previous studies of aged B6 mice have reported numerous changes in the HSC compartment compared with young mice. These include a dramatic increase in the proportion of BM cells with HSC markers and a concomitant decrease in function per purified HSC (Dykstra and de Haan, 2008). Our data extend these earlier findings, documenting a mean 12-fold increase in LSK48−34−E+150+ cell frequency along with a 2.2-fold reduction in functional frequency when measured in a long-term transplantation assay. We also report that the age-related increase in the stem cell pool is highly variable between individual old mice, suggesting a possible loss of pool size control with age, yet appears to be independent of the functional changes that were observed in the old stem cells themselves. We observed an approximately two-fold decrease in the short-term homing ability of old as compared with young LSK48−150+ cells, suggesting that defects in homing may account for much of the decrease of similar magnitude in the in vivo functional frequency of old LSK48−34−E+150+ cells. A similar reduction was also observed in the percentage of purified old cells with CAFC activity in stromal cell–containing co-cultures, although old and young cells had equally high clonogenic efficiency in stroma-free liquid cultures. The finding that these two properties were not shared by the same cells argues against the concept of a discrete nonfunctional subpopulation in old LSK48−34−E+150+ cells, as was suggested previously (Sudo et al., 2000). Rather, it favors a model in which all old LSK48−34−E+150+ cells (and by extension, all old HSCs) are reduced in their ability to respond to a variety of environmental cues. This reduced responsiveness could result in a reduced proportion of old LSK48−34−E+150+ cells that read out in any given assay and could also result in the cells that do read out in the assay exhibiting altered functional properties compared with young HSCs. Our data are consistent with this model, as both quantitative and qualitative functional defects were observed when old LSK48−34−E+150+ cells were assayed in stromal co-cultures and in an in vivo transplant setting.

An important unresolved question in the HSC aging field regards the developmental relationship between the HSC subtypes seen in young mice and the myeloid-dominant HSCs that accumulate with age. Here, using clonal analyses of purified HSCs, we confirm a dramatic increase in aged mice of HSCs

Table I. Summary of secondary transplant results

Age of original donor and 24–wk lineage contribution ratio in primary recipient	Proportion of successful secondary transplants
Young	
Myeloid dominant	9 of 9
Balanced	9 of 9
Lymphoid dominant	2 of 2
Total	20 of 20
Old	
Myeloid dominant	16 of 26
Balanced	8 of 11
Lymphoid dominant	0 of 1
Total	24 of 38

42–52 wk after transplant, BM was harvested from 20 primary recipients of young LSK48−34−E+150+ cells and 38 primary recipients of old LSK48−34−E+150+ cells as shown in Fig. 3 and injected into pairs of secondary recipients. Shown in the table are the success rates (i.e., one or both secondary recipients with >1% donor contribution to circulating Gr-1+SSChi cells at 24 wk) for secondary transplantations from primary recipients of old and young myeloid-dominant, balanced, and lymphoid-dominant HSCs.

that display predominantly myeloid outputs. However, we show that these myeloid-dominant HSCs exhibit multiple functional defects as compared with young myeloid-dominant HSCs. It should be noted that in spite of their functional defects, these cells are still bona fide long-term repopulating HSCs, as indicated by their continued production of short-lived granulocytes at 6 mo after transplant, and their ability to successfully repopulate secondary recipients after 1 yr in

primary recipients. This finding challenges the notion that the myeloid-dominant HSCs that accumulate with age are functionally equivalent to those in young mice (Cho et al., 2008; Muller-Sieburg and Sieburg, 2008). However, it is conceivable that a minor subset of young myeloid-dominant HSCs, functionally equivalent to the low-output myeloid-dominant HSCs in old mice, might expand with age (assuming they had a relative competitive advantage over the rest of the HSC pool).
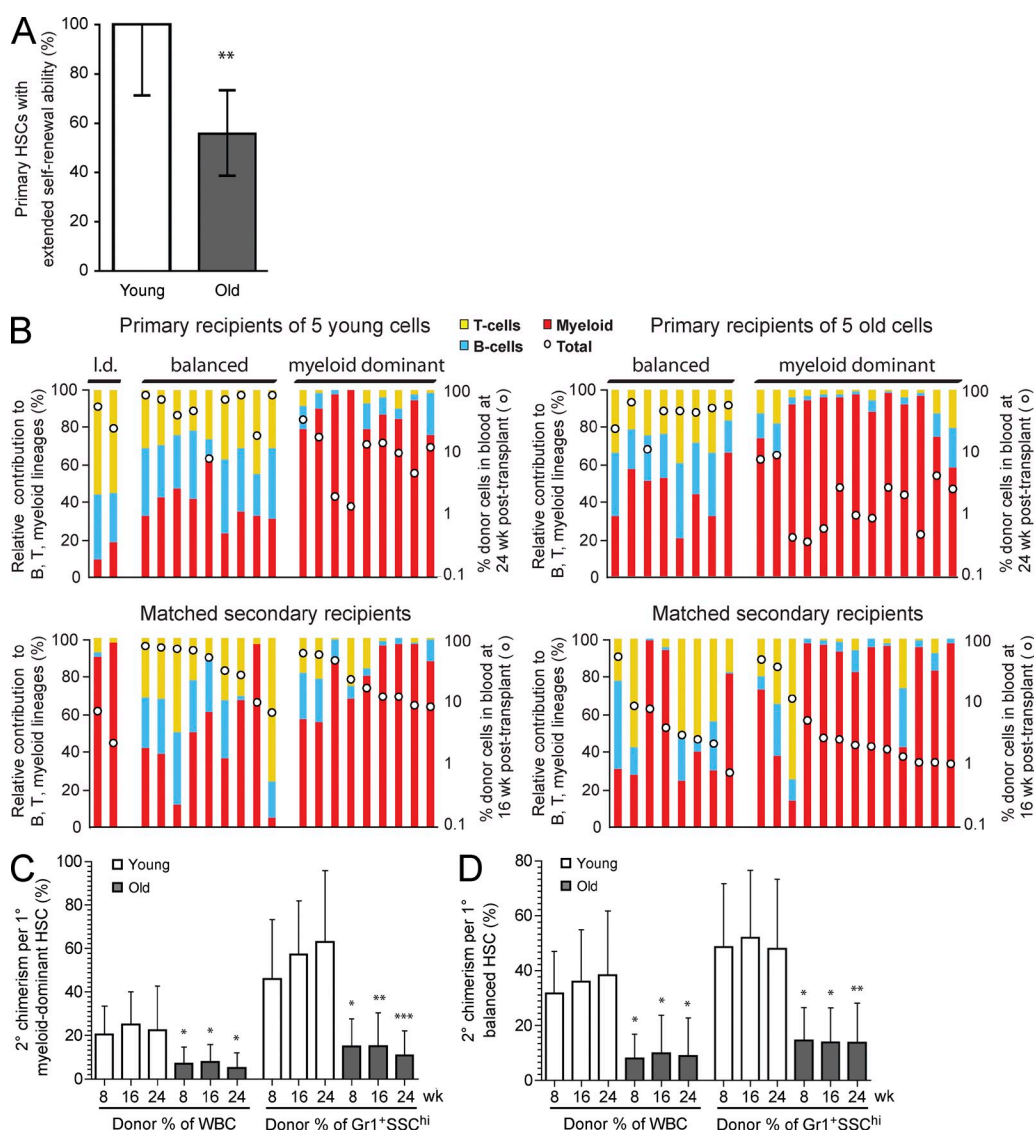
Figure 5. Old HSCs exhibit decreased self–renewal activity and smaller secondary clone size when measured by secondary transplantation in vivo. (A) After correcting for the differences in primary HSC frequencies, the proportion of primary HSCs with extensive in vivo self-renewal activity was calculated based on the secondary transplantation results shown in Table I. **, $P < 0.01$ for corrected proportions (Fishers exact test). Error bars represent corrected 95% confidence interval for original proportions. (B) All positive W41 secondary recipients and their corresponding primary recipients are shown. Colored bars and white dots represent relative donor lineage contribution and absolute donor proportion in the blood, as described for Fig. 3 C. Top panels show individual primary recipients, grouped by relative lineage contribution pattern as in Fig. 3 C. Bottom panels show the positive secondary recipients, arranged so that corresponding primary and secondary recipients are aligned vertically. l.d., lymphoid dominant. (C and D) The mean contribution to total peripheral blood or to the granulocyte lineage in secondary (2°) W41 recipients was calculated per primary (1°) young myeloid-dominant ($n = 9$), young balanced ($n = 9$), old myeloid-dominant ($n = 13$), or old balanced ($n = 8$) HSC by dividing by the mean number of functional HSCs injected per positive primary recipient (1.79 HSCs per positive young recipient and 1.33 HSCs per positive old recipient). Time is shown as weeks after transplant. Error bars represent 95% confidence intervals. *, $P < 0.05$; **, $P < 0.01$; ***, $P < 0.001$, Mann-Whitney U test.

Table II. Summary of tertiary transplant results

Secondary number	Positive proportion of tertiary recipients transplanted with		
	100 LSK48⁻150⁺	40 LSK48⁻150⁺	20 LSK48⁻150⁺
#1	0 of 0	0 of 0	0 of 4
#2	1 of 4	0 of 0	1 of 12
#3	1 of 9	0 of 3	4 of 26
#4	1 of 1	3 of 6	2 of 8
#5	2 of 6	0 of 0	4 of 9
#6	6 of 6	0 of 0	7 of 12
#7	8 of 8	3 of 3	5 of 15

6–12 mo after secondary transplantation of young LSK48⁻34⁻E⁺150⁺ cells, regenerated donor LSK48⁻150⁺ cells were purified from selected positive secondary recipients (#1–#7) and injected at limiting dilutions (20, 40, or 100 cells) into tertiary recipients, as indicated in Fig. 3 and described in Materials and methods. Shown in the table are the proportion of tertiary transplanted animals in which continuing donor-derived hematopoiesis could be detected (>0.5% donor contribution to circulating Gr-1⁺SSCʰⁱ granulocytes at 16–24 wk after transplant). Repopulation details of all positive tertiary recipients and the corresponding primary and secondary recipients are shown in Fig. 6.

In support of this possibility, such HSCs have been reported to exist at low frequency in young mice (Morita et al., 2010) and were observed here also. An alternate possibility is that accumulated DNA damage might be superimposed on the changing HSC pool over time, causing functional deficiencies within the fixed clonal subtypes (Rossi et al., 2007a; Beerman et al., 2010a). In this study, we provide convincing evidence that HSCs undergo qualitative changes as they age by functionally assessing the progeny HSCs of normal young HSCs subjected to extended serial transplantations. From these experiments, we show that low-output myeloid-dominant HSCs similar to those that dominate the HSC compartment in old mice can be derived from robust young myeloid-dominant or balanced HSCs. This observation indicates that these functionally defective HSCs do not represent a fixed subtype and suggest that their accumulation with age is unlikely to be the exclusive result of their selective expansion from HSCs with similar properties that preexist at low frequency in young mice. Accumulated DNA damage superimposed on specific HSC subtypes also seems unlikely. Rather, our findings support a model in which the functional defects characteristic of the HSCs that accumulate in old mice represent age-associated changes that affect the entire HSC pool. This might occur as part of a controlled developmental program or as an end result of somatic evolution within the HSC pool.

The concept that HSC aging might be intrinsically controlled is appealing because the qualitative changes observed in the aging HSC pool are generally consistent between individual mice and appear to occur in a coordinated manner. Recently, Takizawa et al. (2011) reported that HSCs with extensive proliferative history were particularly prone to return to a quiescent state. They further speculated the existence of an intrinsic program that drives cells with high proliferative history toward quiescence. Such a program would explain the accumulation of phenotypic HSCs with age and may be directly related to the functional defects that we observe. Indeed, reduced readout in functional assays, delayed proliferation in stromal cultures, and a reduced clonal output of mature cells in vivo would all be consistent with a heightened degree of enforced quiescence. However, the possible molecular identity of such an intrinsic control mechanism is completely unknown and as such is currently limited only to speculation.

The possibility that HSC aging involves a somatic evolutionary process driven by epigenetic alterations, DNA mutations, and other potential sources of transmitted variability is also of interest. Because most somatic cells have a limited replicative lifespan, somatic evolution at the cell population level is thought to be largely restricted to stem cells (Pepper et al., 2007). Any HSCs with a slightly increased self-renewal ability, increased likelihood of quiescence, and/or decreased response to differentiation signals would tend to remain in the HSC compartment and accumulate there, assuming that these properties would be passed on to their cellular progeny. Conversely, HSCs with different characteristics would be lost. As aging progressed, selective pressures would continue to favor cells with self-renewal ability but not necessarily select for any of the other functional properties of HSCs. As a result, the size of the aged HSC pool would increase, and because of accumulating cellular damage, the functional potential of individual HSCs would decrease. Such cellular aging could thus be a driver of the selection process that ultimately results in the changes in HSC pool composition seen in aged mice. Further support of this concept has been provided from a mathematical modeling perspective, in which the accumulation of division-dependent changes in individual cells has been postulated to be the driving force behind HSC aging (Glauche et al., 2011).

A remaining unresolved question is why the HSCs that become prevalent in aging mice are preferentially myeloid dominant. It is tempting to speculate that some of the transcriptional networks that are required for HSC self-renewal might overlap with myeloid cell production, in contrast to lymphoid cell production which can apparently be lost without affecting self-renewal. One contributing factor to the prevalence of myeloid-dominant HSCs in old mice, shown here by our extended serial transplantation experiments, is that old myeloid-dominant HSCs do not appear to derive exclusively from young myeloid-dominant HSCs.

Figure 6. Low–output myeloid–dominant repopulating cells can be generated from young HSCs in an extended serial transplantation setting. 6–12 mo after transplant, regenerated donor LSK48⁻150⁺ cells were purified from 10 positive secondary recipients, corresponding to 7 positive primary recipients (#1–#7). Purified cells were injected at limiting dilutions (20, 40, or 100 cells) into tertiary recipients, as indicated in Fig. 3 and described in Table II and Materials and methods. Shown here is the donor repopulation kinetics in primary and secondary recipients, as well as all tertiary recipients in which continuing donor-derived hematopoiesis could be detected. Colored bars and white dots represent relative donor lineage contribution and absolute donor proportion in the blood, as described for Fig. 3 C. The groups of four and three bars on the left represent donor blood cell output over time in the primary and secondary recipients, respectively. In cases where pairs of secondary recipients were tested (#2, #3, and #7), the secondary (2°) recipient bars represent the mean donor blood cell output in both secondary mice. The rightmost group of bars represent donor blood cell output in individual positive tertiary (3°) recipients at the time point of final analysis. nd, no donor derived cells detected.

Functional experiments of HSCs at a clonal level as described in this study provide the high resolution that is necessary to address questions about the underlying process of HSC aging and introduce increasing opportunities for new insights into the cellular and molecular mechanisms involved in the aging process. Exciting recent developments in purification and assays for human HSCs (Notta et al., 2011) finally open up the possibility for similar interrogation of the aged human HSC pool at a clonal level. A better understanding of the biology and mechanisms of stem cell aging will help clarify the relationship between the aged HSC pool and hematological diseases of the elderly and could enable targeted treatment strategies aimed to reduce or even reverse the aging process at the stem cell level as a strategy to combat aging and age-related pathologies.

MATERIALS AND METHODS

Mice. Young (4–5 mo) and old (24–26 mo) C57BL/6 (B6) mice were purchased from Harlan and used as BM donors. Recipients were CD45.1 C57BL/6.SJL (B6.SJL) mice obtained from Charles River or bred in-house. C57BL/6J-kit^W-41J/kit^W-41J (W41) mice were obtained from E. Dzerziak (Erasmus Medical Center, Rotterdam, Netherlands) and were crossed with B6.SJL to obtain CD45.1/5.2 W41 heterozygotes and further crossed to obtain CD45.1 W41 homozygotes (W41.SJL). C57BL/6-Tg(CAG-EGFP)1Osb/J (GFP), B6.Cg-Tg(CAG-DsRed*MST)1Nagy/J (dsRed), and B6.129(ICR)-Tg(CAG-ECFP)CK6Nagy/J (CFP) transgenic mice were purchased from the Jackson Laboratory and bred in-house. All experiments were approved by the Animal Experimentation Committee of the University Medical Center Groningen.

Purification and sorting of LSK48⁻34⁻E⁺150⁺ BM cells. Bones (fore and hind limbs, spine, pelvis, sternum, skull, and mandible) were harvested from individual young mice. Hind limbs and pelvises were harvested from individual old mice. After removal of soft tissue, bones were crushed with a mortar and pestle in lysis solution (NH_4Cl) and passed through a 100-µm filter. Cells were washed with PBS + 0.2% BSA and then stained with CD34–FITC, EPCR–biotin, cKit–PE, Sca1–Pacific blue, CD150-PECy7, CD48–Alexa Fluor 647, and Alexa Fluor 700–conjugated lineage antibodies B220, Gr-1, Mac-1, Ter119, CD3 (collectively, Lin–Alexa Fluor 700). After 45 min, cells were washed and secondary stained with streptavidin–conjugated APC-Cy7. After 20 min, cells were washed again and resuspended in 1 µg/ml propidium iodide solution. Cells were double-sorted on a MoFlo Classical and/or MoFlo XDP cell sorter as follows: CD48⁻LSK cells were enriched at high speed using "enrich" mode with a multiple droplet sort envelope, and then LSK48⁻34⁻E⁺150⁺ cells were resorted at low speed using "purify" mode into tubes for limiting dilution injections or "single cell" mode into 60 individual wells of a 96-well plate with preestablished stromal feeder layers for CAFC assay or into individual wells preloaded with 200 µl of media for liquid cultures.

Single-cell CAFC assay. The single-cell CAFC assay was modified from de Haan et al. (1997). The FBMD stromal cell line (originally obtained from R. Ploemacher, Erasmus University, Rotterdam, Netherlands) was maintained in Quantum 333 complete fibroblast medium with ʟ-glutamine (PAA Laboratories) plus 10^{-4} mol/L β-mercaptoethanol, 80 U/ml penicillin, and 80 µg/ml streptomycin at 37°C in a 5% CO_2 incubator. FBMD cells were used to establish stromal cell layers in the inner 60 wells of 96-well microtiter plates and were subsequently incubated at 34°C for the entire culture period. Just before seeding with hematopoietic cells, media was replaced with 200 µl Iscove's modified Dulbecco's medium with GlutaMAX, 20% horse serum, 10^{-5} mol/l hydrocortisone, 10^{-4} mol/l β-mercaptoethanol, 80 U/ml penicillin, and 80 µg/ml streptomycin (collectively, CAFC media). Individual wells were then seeded with single purified cells using the single-cell deposition unit of a MoFlo cell sorter. Each week for up to 13 wk, wells were examined for the presence or absence of cobblestone areas (identified as colonies of at least five

flat nonrefractile cells growing underneath the stromal layer) using 100 magnification on an inverted microscope. Media was also refreshed weekly by removing most of the old media with a suction pipette (without disturbing the stromal layer) and adding 180 µl of fresh CAFC media.

Single-cell liquid cultures. 60–120 purified LSK48$^-$34$^-$E$^+$150$^+$ or LSK48$^-$150$^+$ cells from each of five young or six old mice were individually seeded using the single-cell deposition unit of a MoFlo cell sorter into separate wells of round-bottom 96-well plates containing 200 µl StemSpan media (STEMCELL Technologies) supplemented with 10% FCS, 300 ng/ml of stem cell factor, and 20 ng/ml IL-11. Plates were incubated at 37°C, and 13–14 d later, wells were scored for the presence or absence of a clone of at least 5,000 cells. The proportion of wells containing such clones is reported as the clonogenic efficiency in liquid culture. Note that wells were not checked for the presence or absence of a starting cell, so all wells were assumed to have received one cell.

Limiting dilution transplantations and determination of lineage bias. 60 LSK48$^-$34$^-$E$^+$150$^+$ cells from individual young or old B6 (CD45.2) mice were sorted into 600 µl PBS supplemented with 5% FCS. 6 × 10^6 whole BM cells from CD45.1/5.2 W41 heterozygous mice were added as radioprotective/competitor cells, and total volume was adjusted to 1.2 ml. 100 µl of the resulting cell mixture was injected retroorbitally into groups of up to 10 young B6.SJL (CD45.1) recipients that were lethally irradiated (9.5Gy) 24–30 h previously. In this way, each recipient was transplanted with a mean of five purified cells plus 5 × 10^5 radioprotective/competitor cells. At specified times after transplantation, blood samples were obtained via retroorbital puncture. Erythrocytes were lysed with ammonium chloride solution, and the remaining cells were stained with CD45.1-PE, CD45.2–Pacific blue, B220-FITC, CD3-APC, Gr-1–PECy7, and Mac-1–Alexa Fluor 700. Cells were washed and resuspended in 1 µg/ml propidium iodide solution and analyzed on an LSR-II (BD). Recipients with >1% donor-derived contribution to Gr-1$^+$SSC^{hi} cells at 24 wk after transplant were considered to be repopulated with HSCs and were counted as positive for the purposes of the limiting dilution calculation, performed using the Web-based calculator provided at http://bioinf.wehi.edu.au/software/elda/ (Hu and Smyth, 2009). Relative lineage contribution ratio was determined as follows: A minimum of 100,000 events were collected for each blood sample. Doublets, dead cells, erythrocytes, and debris were excluded using appropriate gates. Myeloid cells were defined as Gr-1− and/or Mac-1–positive events that were negative for CD3 and B220. T cells were defined as CD3-positive events that were negative for B220, Gr-1, and Mac-1. B cells were defined as B220-positive events that were negative for CD3, Gr-1, and Mac-1. The proportion of myeloid (GM), B, and T cells that were donor derived was then determined using CD45.1 versus CD45.2 for each cell type. The donor proportion of each lineage was then plotted relative to each other in a 100% stacked bar graph. Thus, a perfectly balanced donor clone (e.g., contributing 50% of all circulating T cells, 50% of all circulating B cells, and 50% of all circulating myeloid cells in that mouse) would show exactly one-third of the stacked bar for each lineage. The total donor chimerism was determined by dividing the sum of the donor myeloid, B, and T cells by the sum of all myeloid, B, and T cells. Lymphoid-dominant, myeloid-dominant, and balanced HSCs were retrospectively identified by the GM/(B + T) donor contribution ratio at 24 wk after transplant. A GM/(B + T) ratio of <0.25 indicated a lymphoid-dominant HSC, a GM/(B + T) ratio of >2 indicated a myeloid-dominant HSC, and a GM/(B + T) ratio between 0.25 and 2 indicated a balanced HSC. Note that the strategy used here is identical to previously described criteria used to identify α-, β-, γ-, and δ-LTRCs (Dykstra et al., 2007), with two important differences. First, instead of measuring the relative lineage contribution at 16 wk after transplant, we used 24 wk after transplant to determine this ratio. Second, instead of >1% donor-derived cells in the blood at 16 wk after transplant to define a positive recipient, we used >1% donor-derived Gr-1$^+$SSC^{hi} cells at 24 wk after transplant. The criteria used here exclude most or all repopulating cells lacking robust self-renewal potential in young mice (i.e., γ- and δ-LTRCs; Dykstra et al., 2007).

Secondary transplantations of nonseparated BM. 59 primary recipients positive at 24 wk (20 recipients of five young cells and 39 recipients of five old cells) were sacrificed at 10–12 mo after transplant. Hind limbs were harvested, and bones were crushed with a mortar and pestle. Cells were counted, and 5 million BM cells were injected without competitor cells into pairs of recipients: one young B6.SJL recipient lethally irradiated with 9.5 Gy and one young W41.SJL recipient sublethally irradiated with 3.5 Gy. 8, 16, and 24 wk after transplantation, blood samples were collected and analyzed as in the primary recipients. Secondary recipients with >1% donor-derived Gr-1$^+$SSC^{hi} cells at 24 wk after transplant were considered to be evidence for in vivo self-renewal ability in the primary clone.

Tertiary transplantations of donor-derived HSCs. 1–2 secondary recipients from each of 7 selected primary recipients (10 secondary recipients in total) were sacrificed 6–12 mo after transplant, and hind limbs and pelvises were harvested. BM cells obtained by crushing were washed with PBS + 0.2% BSA and then stained with cKit-PE, Sca1–Pacific blue, CD48–Alexa Fluor 647, and Lin–Alexa Fluor 700. CD48$^-$LSK cells were presorted and then restained with additional antibodies to CD45.2-PerCPCy5.5, CD45.1-PECy7, CD150-FITC, and DAPI as a viability stain. CD45.2$^+$CD45.1$^-$CD48$^-$CD150$^+$LSK cells were then sorted into tubes for tertiary transplantations. Dilutions of 20, 40, and/or 100 donor-derived CD45.2$^+$CD45.1$^-$CD48$^-$CD150$^+$LSK cells from each of seven donors were injected into a total of 132 tertiary recipients (58 lethally irradiated B6.SJL [CD45.1] recipients receiving 1.5 million W41.SJL radioprotective cells and 74 sublethally irradiated W41.SJL recipients without radioprotective cells).

Short-term homing experiments. Bones (fore and hind limbs, spine, pelvis, and sternum) were harvested from individual old (27–28 mo) and groups of two young (2.5–3.5 mo) CFP, GFP, or dsRed mice, some of which had been crossed several generations with B6.SJL to acquire the CD45.1 allele. BM cells were obtained by crushing and were stained with CD150-PECy7, CD48–Alexa Fluor 647, Lin–Alexa Fluor 700, cKit-PE or cKit–FITC, and Sca1–Pacific blue or Sca1-FITC. LSK cells were presorted using a MoFlo Classical, and CFP$^+$, GFP$^+$, or dsRed$^+$ LSK48$^-$150$^+$ cells were then resorted using a MoFlo XDP. Single young or old GFP$^+$LSK48$^-$150$^+$ cells were sorted into individual wells of 96-well CAFC plates. The remaining cells (0.3–1.0 × 10^4 young and 0.7–4.4 × 10^4 old LSK48-150$^+$ cells) were combined at known ratios and injected into a single 2–3-mo-old B6 recipient irradiated 24 h previously with 9.5 Gy from a ^{137}Cs source. 16–21 h later, the recipient mouse was sacrificed, and bones (fore and hind limbs, spine, pelvis, and sternum) were harvested, crushed, and stained with CD45.1–Alexa Fluor 647, CD45.2-PECy7, and propidium iodide. The ratio of homed CFP$^+$, GFP$^+$ and/or dsRed$^+$ CD45.1$^+$ or CD45.2$^+$ cells was measured and compared with the ratio of the injected cells to determine the relative homing efficiency. In addition, single cells of each homed type were seeded into individual wells of 96-well CAFC plates to compare the function of the homed cells with the freshly isolated starting population.

Functional defects of aged murine HSCs | Dykstra et al.

REFERENCES

Beerman, I., D. Bhattacharya, S. Zandi, M. Sigvardsson, I.L. Weissman, D. Bryder, and D.J. Rossi. 2010a. Functionally distinct hematopoietic stem cells modulate hematopoietic lineage potential during aging by a mechanism of clonal expansion. *Proc. Natl. Acad. Sci. USA*. 107:5465–5470. http://dx.doi.org/10.1073/pnas.1000834107

Beerman, I., W.J. Maloney, I.L. Weissmann, and D.J. Rossi. 2010b. Stem cells and the aging hematopoietic system. *Curr. Opin. Immunol.* 22:500–506. http://dx.doi.org/10.1016/j.coi.2010.06.007

Bennett-Baker, P.E., J. Wilkowski, and D.T. Burke. 2003. Age-associated activation of epigenetically repressed genes in the mouse. *Genetics*. 165:2055–2062.

Breems, D.A., E.A. Blokland, S. Neben, and R.E. Ploemacher. 1994. Frequency analysis of human primitive haematopoietic stem cell subsets using a cobblestone area forming cell assay. *Leukemia*. 8:1095–1104.

Challen, G.A., N.C. Boles, S.M. Chambers, and M.A. Goodell. 2010. Distinct hematopoietic stem cell subtypes are differentially regulated by TGF-beta1. *Cell Stem Cell*. 6:265–278. http://dx.doi.org/10.1016/j.stem.2010.02.002

Chambers, S.M., C.A. Shaw, C. Gatza, C.J. Fisk, L.A. Donehower, and M.A. Goodell. 2007. Aging hematopoietic stem cells decline in function and exhibit epigenetic dysregulation. *PLoS Biol*. 5:e201. http://dx.doi.org/10.1371/journal.pbio.0050201

Cho, R.H., H.B. Sieburg, and C.E. Muller-Sieburg. 2008. A new mechanism for the aging of hematopoietic stem cells: aging changes the clonal composition of the stem cell compartment but not individual stem cells. *Blood*. 111:5553–5561. http://dx.doi.org/10.1182/blood-2007-11-123547

de Haan, G., W. Nijhof, and G. Van Zant. 1997. Mouse strain-dependent changes in frequency and proliferation of hematopoietic stem cells during aging: correlation between lifespan and cycling activity. *Blood*. 89:1543–1550.

Dykstra, B., and G. de Haan. 2008. Hematopoietic stem cell aging and self-renewal. *Cell Tissue Res*. 331:91–101. http://dx.doi.org/10.1007/s00441-007-0529-9

Dykstra, B., D. Kent, M. Bowie, L. McCaffrey, M. Hamilton, K. Lyons, S.J. Lee, R. Brinkman, and C. Eaves. 2007. Long-term propagation of distinct hematopoietic differentiation programs in vivo. *Cell Stem Cell*. 1:218–229. http://dx.doi.org/10.1016/j.stem.2007.05.015

Glauche, I., L. Thielecke, and I. Roeder. 2011. Cellular aging leads to functional heterogeneity of hematopoietic stem cells: A modeling perspective. *Aging Cell*. 10:457–465. http://dx.doi.org/10.1111/j.1474-9726.2011.00692.x

Harrison, D.E. 1983. Long-term erythropoietic repopulating ability of old, young, and fetal stem cells. *J. Exp. Med*. 157:1496–1504. http://dx.doi.org/10.1084/jem.157.5.1496

Harrison, D.E., C.M. Astle, and M. Stone. 1989. Numbers and functions of transplantable primitive immunohematopoietic stem cells. Effects of age. *J. Immunol*. 142:3833–3840.

Hu, Y., and G.K. Smyth. 2009. ELDA: extreme limiting dilution analysis for comparing depleted and enriched populations in stem cell and other assays. *J. Immunol. Methods*. 347:70–78. http://dx.doi.org/10.1016/j.jim.2009.06.008

Kent, D.G., M.R. Copley, C. Benz, S. Wöhrer, B.J. Dykstra, E. Ma, J. Cheyne, Y. Zhao, M.B. Bowie, Y. Zhao, et al. 2009. Prospective isolation and molecular characterization of hematopoietic stem cells with durable self-renewal potential. *Blood*. 113:6342–6350. http://dx.doi.org/10.1182/blood-2008-12-192054

Kim, M., H.B. Moon, and G.J. Spangrude. 2003. Major age-related changes of mouse hematopoietic stem/progenitor cells. *Ann. N. Y. Acad. Sci*. 996:195–208. http://dx.doi.org/10.1111/j.1749-6632.2003.tb03247.x

Liang, Y., G. Van Zant, and S.J. Szilvassy. 2005. Effects of aging on the homing and engraftment of murine hematopoietic stem and progenitor cells. *Blood*. 106:1479–1487. http://dx.doi.org/10.1182/blood-2004-11-4282

Liu, L., and T.A. Rando. 2011. Manifestations and mechanisms of stem cell aging. *J. Cell Biol*. 193:257–266. http://dx.doi.org/10.1083/jcb.201010131

Mohrin, M., E. Bourke, D. Alexander, M.R. Warr, K. Barry-Holson, M.M. Le Beau, C.G. Morrison, and E. Passegué. 2010. Hematopoietic stem cell quiescence promotes error-prone DNA repair and mutagenesis. *Cell Stem Cell*. 7:174–185. http://dx.doi.org/10.1016/j.stem.2010.06.014

Morita, Y., H. Ema, and H. Nakauchi. 2010. Heterogeneity and hierarchy within the most primitive hematopoietic stem cell compartment. *J. Exp. Med*. 207:1173–1182. http://dx.doi.org/10.1084/jem.20091318

Morrison, S.J., A.M. Wandycz, K. Akashi, A. Globerson, and I.L. Weissman. 1996. The aging of hematopoietic stem cells. *Nat. Med*. 2:1011–1016. http://dx.doi.org/10.1038/nm0996-1011

Muller-Sieburg, C., and H.B. Sieburg. 2008. Stem cell aging: Survival of the laziest? *Cell Cycle*. 7:3798–3804. http://dx.doi.org/10.4161/cc.7.24.7214

Müller-Sieburg, C.E., R.H. Cho, M. Thoman, B. Adkins, and H.B. Sieburg. 2002. Deterministic regulation of hematopoietic stem cell self-renewal and differentiation. *Blood*. 100:1302–1309.

Neben, S., P. Anklesaria, J. Greenberger, and P. Mauch. 1993. Quantitation of murine hematopoietic stem cells in vitro by limiting dilution analysis of cobblestone area formation on a clonal stromal cell line. *Exp. Hematol*. 21:438–443.

Notta, F., S. Doulatov, E. Laurenti, A. Poeppl, I. Jurisica, and J.E. Dick. 2011. Isolation of single human hematopoietic stem cells capable of long-term multilineage engraftment. *Science*. 333:218–221. http://dx.doi.org/10.1126/science.1201219

Pepper, J.W., K. Sprouffske, and C.C. Maley. 2007. Animal cell differentiation patterns suppress somatic evolution. *PLOS Comput. Biol*. 3:e250. http://dx.doi.org/10.1371/journal.pcbi.0030250

Pillay, J., I. den Braber, N. Vrisekoop, L.M. Kwast, R.J. de Boer, J.A. Borghans, K. Tesselaar, and L. Koenderman. 2010. In vivo labeling with 2H2O reveals a human neutrophil lifespan of 5.4 days. *Blood*. 116:625–627. http://dx.doi.org/10.1182/blood-2010-01-259028

Ploemacher, R.E., J.P. van der Sluijs, C.A. van Beurden, M.R. Baert, and P.L. Chan. 1991. Use of limiting-dilution type long-term marrow cultures in frequency analysis of marrow-repopulating and spleen colony–forming stem cells in the mouse. *Blood*. 78:2527–2533.

Rossi, D.J., D. Bryder, J.M. Zahn, H. Ahlenius, R. Sonu, A.J. Wagers, and I.L. Weissman. 2005. Cell intrinsic alterations underlie hematopoietic stem cell aging. *Proc. Natl. Acad. Sci. USA*. 102:9194–9199. http://dx.doi.org/10.1073/pnas.0503280102

Rossi, D.J., D. Bryder, J. Seita, A. Nussenzweig, J. Hoeijmakers, and I.L. Weissman. 2007a. Deficiencies in DNA damage repair limit the function of haematopoietic stem cells with age. *Nature*. 447:725–729. http://dx.doi.org/10.1038/nature05862

Rossi, D.J., D. Bryder, and I.L. Weissman. 2007b. Hematopoietic stem cell aging: mechanism and consequence. *Exp. Gerontol*. 42:385–390. http://dx.doi.org/10.1016/j.exger.2006.11.019

Sudo, K., H. Ema, Y. Morita, and H. Nakauchi. 2000. Age-associated characteristics of murine hematopoietic stem cells. *J. Exp. Med*. 192:1273–1280. http://dx.doi.org/10.1084/jem.192.9.1273

Takizawa, H., R.R. Regoes, C.S. Boddupalli, S. Bonhoeffer, and M.G. Manz. 2011. Dynamic variation in cycling of hematopoietic stem cells in steady state and inflammation. *J. Exp. Med*. 208:273–284. http://dx.doi.org/10.1084/jem.20101643

Wilson, A., E. Laurenti, G. Oser, R.C. van der Wath, W. Blanco-Bose, M. Jaworski, S. Offner, C.F. Dunant, L. Eshkind, E. Bockamp, et al. 2008. Hematopoietic stem cells reversibly switch from dormancy to self-renewal during homeostasis and repair. *Cell*. 135:1118–1129. http://dx.doi.org/10.1016/j.cell.2008.10.048

Yahata, T., T. Takanashi, Y. Muguruma, A.A. Ibrahim, H. Matsuzawa, T. Uno, Y. Sheng, M. Onizuka, M. Ito, S. Kato, and K. Ando. 2011. Accumulation of oxidative DNA damage restricts the self-renewal capacity of human hematopoietic stem cells. *Blood*. 118:2941–2950. http://dx.doi.org/10.1182/blood-2011-01-330050

Yilmaz, O.H., M.J. Kiel, and S.J. Morrison. 2006. SLAM family markers are conserved among hematopoietic stem cells from old and reconstituted mice and markedly increase their purity. *Blood*. 107:924–930. http://dx.doi.org/10.1182/blood-2005-05-2140